

Title No. 121-M05

High-Volume Fly Ash Engineered Cementitious Composite for Underground and Hydraulic Engineering

by Xiaoqin Li, Li Zhang, Wenlu Wen, Shihua Li, and Xu Zhou

Engineered cementitious composites (ECCs) have excellent toughness and crack-control abilities compared to other cement-based materials, which can be used in underground and hydraulic engineering. Nevertheless, excellent impermeability and workability and low drying shrinkage are also required. Two groups of ECC mixture proportions with high fly ash-cement (FA/c) and water-cement ratios (w/c) were chosen as baselines, and silica fume (SF) and a shrinkage-reducing agent (SRA) were introduced to improve the impermeability, workability, and mechanical behaviors. The workability laboratory evaluation indexes of ECC were also discussed. ECC mixture proportions with excellent workability (pumpability and sprayability), high toughness (ultimate tensile strain ϵ_{tp} over 3.5%), good impermeability (permeability coefficient $K = 1.713 \times 10^{-11}$ m/s), and low drying shrinkage (drying shrinkage strain $\epsilon_{st} = 603.6 \times 10^{-6}$) were finally obtained. Then, flexural and shear tests were carried out for the material flexural/shear strength and toughness evaluations, giving the characteristic material properties for the final ECC mixture proportions.

Keywords: engineered cementitious composite (ECC); high-volume fly ash; impermeability; low drying shrinkage; toughness; workability.

INTRODUCTION

The importance of controlling crack width has gained much attention in underground and hydraulic engineering. Normal concrete (NC) behaves brittlely, with poor crack-control abilities due to its low toughness, of which the ultimate tensile strain is only approximately 0.01% and the relevant NC local crack width may exceed 0.6 mm.^{1,2} Due to the low toughness and poor crack-control abilities, underground tunnel lining deterioration, spalling of concrete debris, and water leakages may occur, especially when the tunnel is exposed to an aggressive environment.^{3,4} Nevertheless, for hydraulic structures, including dams, spillways, and sluices, concrete cracking may also induce structural damage.^{5,6} To solve these problems, engineered cementitious composites (ECCs) could be introduced, which exhibit strain-hardening behavior under uniaxial tensile loading conditions. The tensile strain capacity of ECC ranges from 3 to 7%, which is 300 to 700 times that of NC.⁷ More importantly, the high tensile ductility of ECC is achieved by forming multiple tight microcracks instead of large localized cracks,^{5,7} and the crack width is typically less than 80 μm , even when the tensile strain is up to 5%.⁸ Also, the cement industry accounts for 5 to 8% of worldwide CO₂ emissions, and approximately 0.94 tons of CO₂ are released into the atmosphere while manufacturing 1 ton of cement.^{9,10} Industrial by-product fly ash (FA) can replace a large portion of cement in ECC to enhance tensile ductility⁹ and also offers environmental

advantages compared to processing cement, such as reducing the energy investment and CO₂ release.¹¹ Aggregates with sizes larger than average fiber spacing can cause poor fiber dispersion, which leads to a reduction in the number of effective fibers at the failure crack, resulting in a decrease in tensile strength. As the particle size of FA is less than 10 μm , which is much smaller than average fiber spacing, adding FA can improve fiber dispersion homogeneity in the fresh state and also improve ECC tensile ductility.¹² Moreover, it was pointed out by Şahmaran and Li¹³ that for high-volume FA ECC, the crack width may be reduced to 10 to 30 μm , sometimes even lower than 10 μm —much smaller than the 80 μm discussed earlier⁸—which is beneficial to the structural durability, too.

Based on its excellent mechanical properties and advantages in reducing CO₂ emissions, high-volume FA ECC has been extensively investigated for repairing waterproofing structures, such as bridges,¹⁴ dams,¹⁵ and tunnels.¹⁶ When a large amount of ECC needs to be applied in new building structures, the pumpability and sprayability are required. However, few research studies have given a detailed discussion on ECC workability, and little attention has been paid regarding the proper laboratory evaluation indexes for ECC. In addition, for ECC used in underground and hydraulic engineering, high impermeability is also required, which is of crucial importance to the material durability.¹⁷ Nevertheless, to obtain ECC that exhibits desirable pseudo-strain-hardening behavior and improved elastic modulus, only a small amount of fine sand is allowed to be applied in the matrix to control fracture toughness.¹⁸ As a result of this requirement, a high drying shrinkage strain may develop during setting and hardening of the composite,¹⁹ which is not expected in underground and hydraulic engineering as it may induce lining cracks, cavities in tunnel linings, and water leakage. Based on the previous discussions, the impermeability, workability, drying shrinkage strain, and mechanical properties for high-volume FA ECC, as well as proper workability laboratory evaluation indexes, should be comprehensively evaluated before being used in underground and hydraulic engineering.

Generally, the permeability coefficient K is required to be less than 2.610×10^{-11} m/s for underground and hydraulic

ACI Materials Journal, V. 121, No. 1, January 2024.

MS No. M-2022-296.R1, doi: 10.14359/51739200, received June 26, 2023, and reviewed under Institute publication policies. Copyright © 2024, American Concrete Institute. All rights reserved, including the making of copies unless permission is obtained from the copyright proprietors. Pertinent discussion including author's closure, if any, will be published ten months from this journal's date if the discussion is received within four months of the paper's print publication.

Table 1—Investigated ECC mixture proportions (mass ratios to cement)

	No.	Cement	FA (Class F)	Water	Sand	HRWRA	PVA fiber	SF	SRA
E-1	E-1.0	1	1.72	1.03	0.7	0.006	0.055	0	0
	E-1.1	1	1.72	1.03	0.7	0.006	0.055	0.10	0.09
	E-1.2	1	1.72	1.03	0.7	0.006	0.055	0.15	0.09
	E-1.3	1	1.72	1.03	0.7	0.006	0.055	0.20	0.09
E-2	E-2.0	1	4.44	1.55	1.11	0.024	0.111	0.10	0.09
	E-2.1	1	4.44	1.55	1.11	0.024	0.111	0.15	0.09
	E-2.2	1	4.44	1.55	1.11	0.024	0.111	0.20	0.09

applications.²⁰ The impermeability is mainly related to its fiber content²¹ and porosity.²² The fiber content of ECC is typically close to or less than 2% by volume, which indicates that the effect of fiber content is small. The porosity of cement-based materials is usually related to the particle size of coarse aggregates,²³ mineral admixtures,^{24,25} and the water-cement ratio (w/c).^{22,26,27} Regardless of coarse aggregates, the effects of aggregate on porosity should not be considered for ECC. Therefore, mineral admixtures and w/c should be considered. According to existing research—for example, the test done by Ding et al.²⁸—the optimal ECC mixture proportions²⁹ with a low w/c (0.57) could not satisfy the workability requirements, including pumpability and sprayability, which could not be easily improved. Although a high w/c might lead to poor impermeability, it could be improved by adding the by-product of the ferrosilicon industry, silica fume (SF), and other additional agents. Moreover, as the particle size of FA is less than 10 μm , it can be used as the filler to improve pore distributions and reduce porosity,²⁴ thereby reducing permeability. As there is no coarse aggregate in ECC, shrinkage-reducing agents (SRAs) should be introduced to reduce drying shrinkage by reducing the surface tension of concrete's fluid, resulting in a significant reduction of the magnitude of capillary stresses and shrinkage strains that occur when concrete loses moisture.³⁰ Adding SRAs could not only obtain a material with a low drying shrinkage strain, but also reduce the quantity of detrimental pores (pore diameter $d > 200$ nm) and increase the number of innocuous pores (pore diameter $d < 20$ nm), which is beneficial to the denseness of the inner paste structure and can improve the resistance to chemical attack and the durability of cement-based materials.³¹

Based on the previous discussions, high-volume FA ECC mixture proportions with high w/c should be adopted as the baselines to conduct empirical research rather than those with low w/c , and SF and SRA needed to be introduced. The influences of w/c , FA, SF, and SRA to the ECC material properties should be carefully investigated, giving the optimum ECC mixture proportions for underground and hydraulic engineering to have excellent mechanical behavior, the required workability, high impermeability, and low drying shrinkage strain. Also, the proper workability laboratory evaluation indexes that can be used to indirectly predict the quality of spraying need to be given. Moreover, the toughness evaluation and material characteristic parameters calibration should be carried out for the final optimized ECC.

RESEARCH SIGNIFICANCE

ECC has excellent toughness and crack-control abilities compared to other cement-based materials, which could be used in underground and hydraulic engineering to prevent tunnel lining deterioration, spalling of concrete debris, water leakages, and so on. Industrial by-product FA can be introduced to ECC to replace a large amount of cement, which can not only benefit the environment but also could enhance its tensile ductility. When a large amount of ECC needs to be applied in underground and hydraulic engineering, the pumpability and sprayability of ECC are required. Specifically, the significance of this investigation lies in optimizing a high fly ash-cement mass ratio (FA/c) and high w/c ECC mixture proportions with good workability (pumpability and sprayability) and impermeability and low drying shrinkage for underground and hydraulic engineering, and establishing proper workability laboratory evaluation indexes for ECC that can be used to indirectly predict the quality of spraying.

EXPERIMENTAL DESIGN

ECC mixture proportions design

To obtain ECC mixture proportions with excellent mechanical properties, impermeability, and workability, two ECC mixture proportions with high FA/c (1.72, 4.44) and w/c (1.03, 1.55)²⁹ were chosen as the baselines, which were named E-1.0 and E-2.0, respectively, in Table 1, of which the ultimate tensile strain ϵ_{tp} is over 3%. SF, with its high content of glass-phase silicon dioxide (SiO_2), consists of very small spherical particles that could be added to ECC mixture proportions to solve the problem of the early-strength reduction that results from adding high-volume FA due to its slow pozzolanic reactivity.²¹ Adding SF aids pumping by reducing torque viscosity while also providing enhanced sprayability by maintaining an appropriate level of flow resistance so that the balance between fluidity and cohesion of fresh cement-based materials can be obtained for better pumpability and sprayability.³² The suggested SF-cement mass ratio (SF/c) was in the range of 8 to 20%³²; therefore, three SF/c —10%, 15%, and 20%—were investigated. As suggested by Gao et al.,¹⁹ when the SRA-cement mass ratio (SRA/c) was 9%, the drying shrinkage strain of ECC might meet the requirements of NC in engineering. The 9% SRA/c was chosen to improve the ECC's anti-drying-shrinkage ability. The investigated ECC mixture proportions are listed in Table 1.

Table 2—Physical properties of P.O 42.5 portland cement

Physical properties	Loss on ignition (LOI), %	Specific surface, m ² /kg	Specific gravity
P.O 42.5 portland cement	1.38	368	3.15

Table 3—Chemical properties of P.O 42.5 portland cement

Mineral composition	SiO ₂	Fe ₂ O ₃	Al ₂ O ₃	CaO	MgO	SO ₃
Mass percent, %	20.8	3.6	4.62	61.61	2.12	2.71

Table 4—Material properties of cement

	Compressive strength, MPa		Bending strength, MPa	
	3 days	28 days	3 days	28 days
Curing time	3 days	28 days	3 days	28 days
Specified value	≥17.0	≥42.5	≥3.5	≥6.5
Actual value	18.9	45.3	4.2	7.8

Raw materials

Materials used to prepare ECC mixtures include P.O 42.5 portland cement, SF, FA (Class F), quartz sand with the particle size ranging from 0.2 to 0.4 mm, water, high-range water-reducing admixture (HRWRA), polyvinyl alcohol (PVA) fibers, and SRA (I). Detailed information of the materials is listed in Tables 2 to 6.

Experimental research

The workability, impermeability, mechanical properties, and drying shrinkage tests were conducted based on the ECC mixture proportions mentioned in Table 1. All specimens were stored for 24 hours at room temperature before demolding, then cured in a standard curing room with a temperature of 20 ± 2°C and a humidity of 95% for 28 days.

Workability investigation—The workability of fresh cement-based materials, including pumpability and sprayability, is related to the material fluidity and cohesion. Generally, pumpable materials require high fluidity and low cohesion, and the slump (S_L) is usually used to evaluate the fluidity of cement-based materials, which needs to be controlled in the range of 140 to 200 mm.^{33,34} The slump flow (S_f) and funnel flow time (t) of the pumpable concrete are used as the laboratory evaluation indexes for cohesion evaluation, of which S_f should be in the range of 400 to 600 mm, and the required range of t is 4 to 10 seconds.³⁵ The sprayability additionally requires that, once a fresh cement-based material is sprayed onto the surface of the substrate, it should be viscous enough to stay adhered to the substrate and remain cohesive without composite ingredient segregation.³⁶ The S_L of freshly sprayable materials should be controlled in the range of 100 to 200 mm.³⁵ Meanwhile, the sprayability decreases with the increase in fluidity and increases with cohesion, indicating that a sprayable ECC needs to maintain a balance between fluidity and cohesion.³⁷ To achieve a balance between fluidity and cohesion, the ratio of slump to slump flow (S_L/S_f) of fresh ECC with good workability is approximately 0.45.³⁸ The workability requirements for

Table 5—Material properties of FA (Class F) and SF

Material properties	FA (Class F)	SF
Amount retained on 45 μm sieve, %	8.10	—
Specific gravity	2.51	2.24
LOI, %	4.22	1.98
Moisture content, %	0.80	0.40
Water required, percent of control, %	90.00	121.00
Mass fraction of SiO ₂ , %	55.08	94.00
Mass fraction of Al ₂ O ₃ , %	28.40	0.60
Mass fraction of Fe ₂ O ₃ , %	4.54	0.90

Table 6—Material parameters of PVA fiber

Tensile strength, MPa	Elastic modulus, GPa	Length, mm	Diameter, μm	Density, g/cm ³	Elongation, %
1620	42.8	12	39	1.3	7

Table 7—Workability requirements for pumpable and sprayable fresh ECC

Evaluations	Fluidity	Cohesion		
		Indexes	S_f , mm	t , seconds
Required range	140 to 200	400 to 600	4 to 10	0.450

fresh ECC with good pumpability and sprayability are given in Table 7.

The slump, slump flow, and funnel flow tests were carried out for all of the fresh ECC listed in Table 1,^{35,39} and the data were compared with the requirements in Table 7. For the slump and slump flow tests, the fresh ECC was evenly placed into the slump barrel in three installments and vibrated with a vibrator. The slump barrel was lifted steadily, and the lifting process was controlled in 3 to 7 seconds. When the ECC no longer slumped or the slump time reached 30 seconds, the vertical distance between the slump barrel and the top surface of ECC was measured and reported as the ECC S_L in mm, and the test was completed in 150 seconds. When the fresh ECC no longer slumped or the slump time reached 50 seconds, the two corresponding diameters of the flowed fresh ECC were measured in two orthogonal directions. The S_f in mm of ECC is the average value of the two diameters, and the test was completed in 4 minutes. For the funnel flow test, the slump barrel was inverted on the bracket and the sealing cover was closed. The fresh ECC was put into the slump barrel and vibrated with a vibrator until it was uniformly distributed. Then, the sealing cover was opened, and a timer was used to measure the time interval between opening the sealing cover and ECC emptying from the slump barrel. The funnel flow test operation was taken twice, and the average value of the measured time intervals was the funnel flow time (t) in seconds.

Impermeability—Cylindrical ECC specimens sized Φ175 x 150 x Φ185 mm were made and cured for 27 days to conduct the ECC impermeability tests according to GB/T 50082-2009.⁴⁰ The specimens were sealed with paraffin and kept standing for 1 day before impermeability tests, where

the specimens were fixed onto the concrete permeability apparatus.

The water pressurizing process of the concrete permeability apparatus took no more than 5 minutes, and the timing was started as soon as the proposed water pressure was reached. The water pressure was controlled at 1.2 ± 0.5 MPa within 24 hours, and the tested specimens were removed and then split in half lengthwise to determine the water penetration height. The average penetration height of water D_m was taken from 10 equidistant spots along each face of the split specimen, and K (m/s) could be calculated according to Eq. (1)

$$K = aD_m^2/2TH \quad (1)$$

where D_m is the average penetration height of water, m; H is the water pressure, where 1 MPa is expressed as a height of 102 m, m; T is the constant pressure time, seconds; and a is the water absorption rate, which is generally taken as 0.03. K is required to be less than 2.610×10^{-11} m/s for underground and hydraulic applications.²⁰

Mechanical properties—Cubic specimens sized 100 mm were used for uniaxial compression tests. The compression tests were performed on a 1000 kN-capacity servo-hydraulic universal testing system with controlled monotonic loading, with a speed of 0.15 mm/min for obtaining the compressive strength (f_c). The 330 mm long x 60 mm wide x 15 mm thick dumbbell-shaped specimens were used in the uniaxial tensile tests, shown in Fig. 1, and the tests were carried out on the electro-servo universal testing machine to obtain the tensile strain (ϵ_t) and tensile stress (σ_t). Monotonic loading and displacement control with a speed of 0.15 mm/min were used in the uniaxial tensile tests.

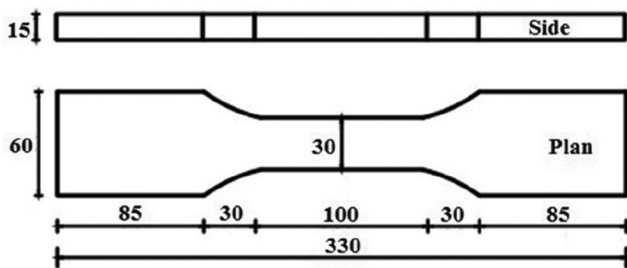


Fig. 1—Dumbbell specimens for ECC direct tension tests (mm).

Table 8—Test results of ECC performance evaluation indexes

No.	Workability (pumpability and sprayability)				Mechanical properties			Impermeability	Drying shrinkage
	S_L , mm	S_t , mm	t , seconds	S_t/S_L	f_c , MPa	ϵ_{sp} , %	σ_{sp} , MPa	$K \times 10^{-11}$, m/s	$\epsilon_{st} \times 10^{-6}$
E-1.0	218☑	608☑	3.41☑	0.361☑	34.23	3.73	3.25	3.189☑	1021.3☑
E-1.1	197☑	543☑	4.23☑	0.363☑	37.85	3.45	3.46	2.358☑	945.2☑
E-1.2	188☑	436☑	5.38☑	0.432☑	38.42	3.16	3.78	1.912☑	739.1☑
E-1.3	183☑	387☑	5.46☑	0.473☑	38.63	2.98	4.11	1.657☑	811.4☑
E-2.0	188☑	458☑	5.33☑	0.410☑	36.90	4.41	3.48	2.227☑	835.6☑
E-2.1	178☑	425☑	5.48☑	0.418☑	41.18	4.02	3.92	1.902☑	846.5☑
E-2.2	174☑	412☑	5.73☑	0.423☑	43.67	3.80	4.12	1.713☑	603.6☑

Note: ☑ stands for test results satisfy requirements; ☒ stands for test results do not satisfy requirements.

Drying shrinkage tests—Specimens of 100 x 100 x 510 mm and a horizontal length comparator with a 540 mm survey scaled distance and 0.001 mm resolution were used for drying shrinkage tests.⁴⁰ The shrinkage tests were performed at a room temperature of $20 \pm 2^\circ\text{C}$ and relative humidity of $60 \pm 5\%$. The length of the specimens during the curing time was measured, and the drying shrinkage strain ϵ_{st} could be calculated based on Eq. (2)

$$\epsilon_{st} = (L_0 - L_t)/L_b \quad (2)$$

where L_0 is the length of the specimen at the beginning, mm; L_t is the length of the specimen after 28 days, mm; and L_b is 540 mm. The resolution of ϵ_{st} should be 1.0×10^{-6} . The 28-day drying shrinkage strain ϵ_{st} of cement-based materials used in underground and hydraulic practical engineering should be lower than 800×10^{-6} .⁴¹

ECC MIXTURE PROPORTIONS OPTIMIZATION BASED ON TEST RESULTS

General test results

Based on the workability, impermeability, and drying shrinkage requirements listed in the “Experimental research” section, the empirical results are evaluated in Table 8.

Test results discussion and analysis

Mechanical properties—According to Table 8, the f_c were all over 30 MPa, of which the f_c of E-2.2 achieved 43.67 MPa. The tensile stress-strain curves of each group are shown in Fig. 2, and it could be observed clearly that each group had obvious strain hardening, and the ultimate tensile strain was in the range of 3.25 to 4.12%.

The mechanical properties of the E-1 and E-2 series were all good, but the workability and impermeability of the specimens were quite different from each other, which are of crucial importance when a large amount of ECC is applied in underground and hydraulic engineering. Therefore, the effects of adding SF to ECC workability and impermeability need to be further discussed.

Workability—The relationship between SF content and workability evaluation indexes (slump, slump flow, flow time, and the S_t/S_L) of the E-1 and E-2 series is shown in Fig. 3.

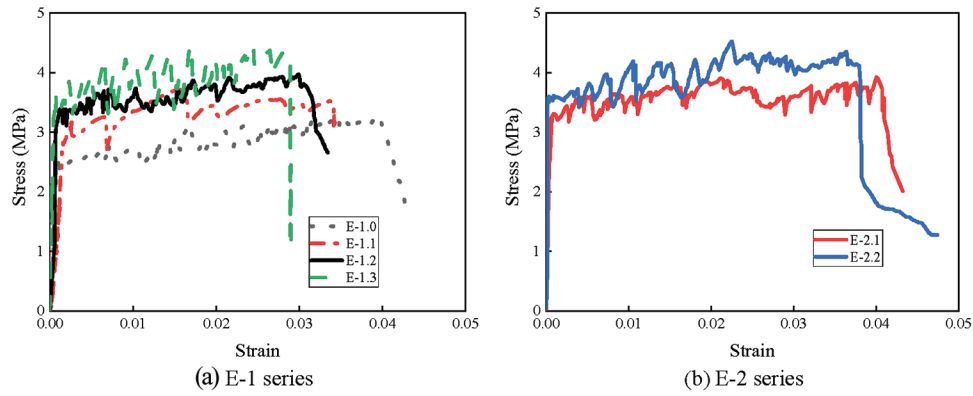


Fig. 2—Tensile stress-strain curves.

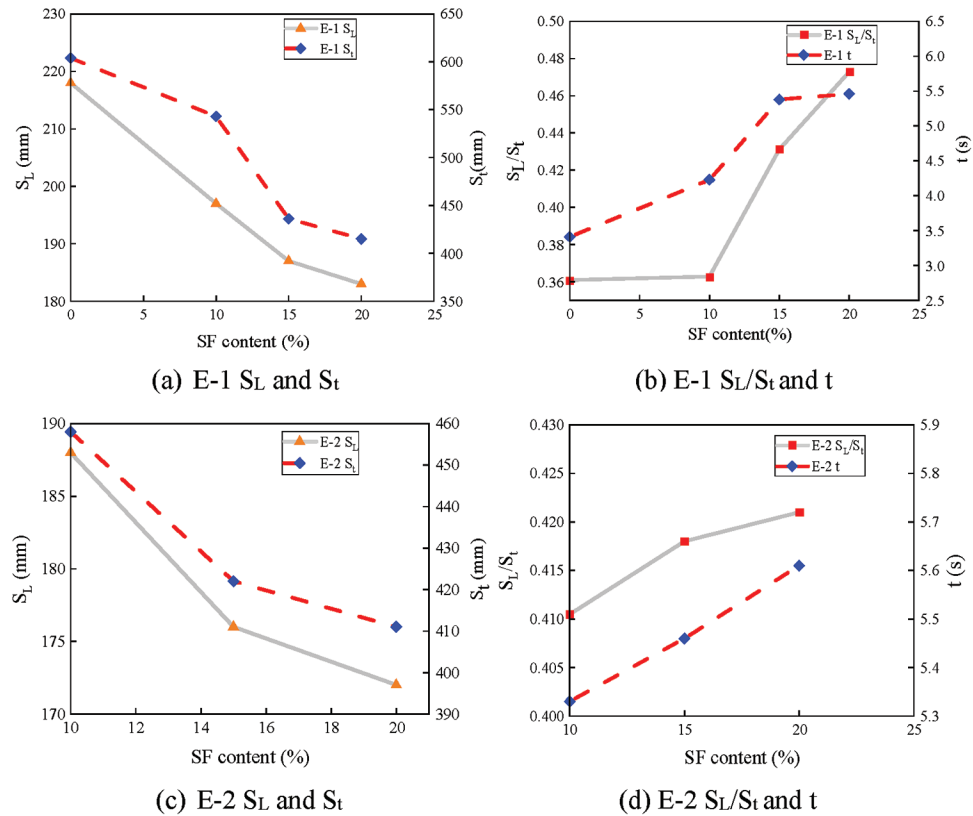


Fig. 3—Relationships between SF content and workability evaluation indexes.

It can be seen from Fig. 3 that the S_L decreased gradually with the increase in SF content, indicating that the fluidity decreased as the amount of SF increased. However, the S_t decreased and the t increased as SF was added, indicating that the cohesion increased with the increase in SF. For the E-1 series, the S_L of E-1.0 was 218 mm, which exceeded the upper limit of S_L (200 mm) according to Table 7. The S_t of E-1.3 is only 387 mm, which cannot satisfy the required lower limit 400 mm. The S_L , S_t , and t of groups E-1.1 and E-1.2 were in the required ranges. In addition, the S_L/S_t of E-1.2 was 0.432, which was closer to 0.450. For the E-2 series, the S_L , S_t , and t were all within the required range. In addition, the S_L/S_t of E-2.2 was 0.423, which was the closest to the suggested 0.450. The use of SF can effectively improve both the pumpability and sprayability of high- w/c ECC. The extremely fine SF particles can improve sprayability in a pozzolanic admixture by maintaining proper cohesion and

increasing the thickness of sprayed cement-based materials, minimizing the rebound degree.³⁷ At the same time, fine SF can help form a lubricating layer on the surface of the mixture, resulting in reduced pumping resistance, which has a positive effect on pumpability.

Impermeability—The average permeability height H and the K of each group are listed in Table 9. It can be observed that as more SF was added, lower H and K values were achieved. The SF hydrated with the cement, which improved the microstructure uniformity and reduced the ECC's porosity by forming additional calcium silicate hydrate (C-S-H).³² Also, adding SF might increase the density of the cement matrix. For the E-2 series, the impermeability was better than that of the E-1 series under the same SF mass ratio—even their w/c were close to each other—because FA mass ratios were higher for the E-2 series, and plenty of C-S-H was produced through pozzolanic reactions, making

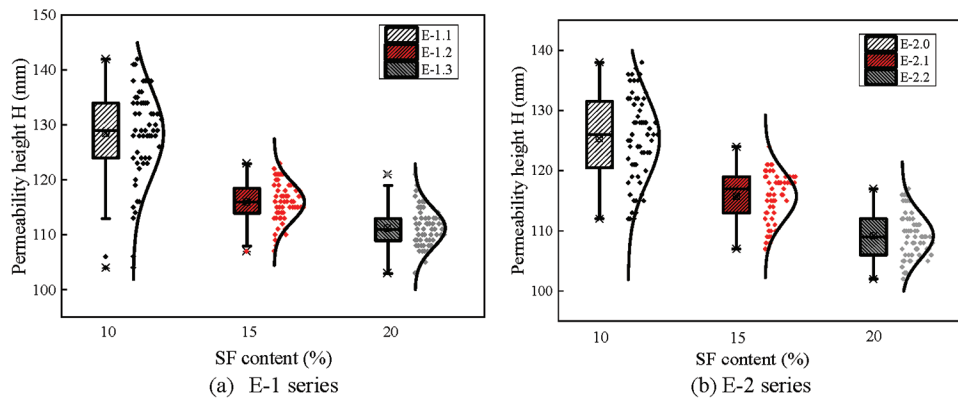


Fig. 4—Box plots for relationships between SF content and H.

Table 9—Average H and K of each group

Series	No.	H, m	$K \times 10^{-11}$, m/s
E-1	E-1.0	148.9	3.189
	E-1.1	128.9	2.358
	E-1.2	116.1	1.912
	E-1.3	108.1	1.657
E-2	E-2.0	125.3	2.227
	E-2.1	115.8	1.902
	E-2.2	109.9	1.713

the cement matrix denser and the pores finer. Meanwhile, the pozzolanic reaction takes some of the free water in the system, which indirectly reduces the porosity.⁴²

Box plots were used to analyze the dispersion of each group's H, as shown in Fig. 4. It was found that the median and average values of H of E-1 were nearly located at the middle of the box plot. The H distributions of E-1.2 and E-1.3 were closer to normal distributions compared with E-1.1. However, for E-1.3, there was an exceptional datum, and the H was higher, indicating poor impermeability. Although E-1.2 also has an exceptional datum, it was with a lower H, indicating good impermeability. It can be seen from Fig. 4(b) that the H distribution of E-2.2 was closer to the normal distributions compared with E-2.0 and E-2.1. The median and average values of H for E-2.2 were nearly located at the middle of the box plot.

To further explore the influence of SF on ECC impermeability, the porosity of the E-1 and E-2 series was analyzed, and the relationship between SF content and porosity was obtained accordingly. Scanning electron microscopy (SEM) was used to investigate the porosity of the E-1 and E-2 series. The 3 x 3 x 1 mm specimens for SEM were obtained from the compressive strength tests and coated with gold using a coating machine to progress the characteristics of electricity transmission. The SEM images were taken at 1000 magnification levels to observe the porosity of ECC and are shown in Fig. 5. Based on the image processing software used, microscopic parameters such as the area and the number of pores were extracted. The porosity was obtained by dividing the area of the pores by the total area. The ECC porosity and pore density of each group are listed in Table 10.

Table 10—Porosity and pore density test results

Series	No.	Pore density, psc./ μm^2	Porosity, %
E-1	E-1.0	0.017	15.43
	E-1.1	0.013	12.76
	E-1.2	0.011	9.31
	E-1.3	0.009	7.16
E-2	E-2.0	0.012	12.01
	E-2.1	0.009	8.99
	E-2.2	0.007	6.98

Note: psc is pore space.

It can be seen from Table 10 that the ECC porosity and pore density decreased with the increase in SF content. The higher the SF/c used, the lower the porosity and pore density. It is well known that the durability of cement-based materials largely depends on the possibility of penetration of hazardous ions into the material with water as the medium.¹⁷ Therefore, combined with the aforementioned test results, adding SF might also improve ECC durability.

ECC mixture proportions optimization

Based on Table 8 and the discussion of the test results, E-1.2 and E-2.2 satisfy the workability evaluation indexes for underground and hydraulic engineering, of which the S_L is in the range of 140 to 200 mm to ensure proper fluidity, the S_t is in the range of 400 to 600 mm, the t should be in the range of 4 to 10 seconds to ensure cohesion, and the S_L/S_t is generally approximately 0.45 to ensure the balance between fluidity and cohesion. Also, for E-1.2 and E-2.2, the ultimate tensile strain ϵ_{tp} was greater than 3%, K was lower than 2.610×10^{-11} m/s, and drying shrinkage strain ϵ_{st} was lower than 800×10^{-6} .

To optimize the final ECC mixture proportions, spray tests were carried out on E-1.2 and E-2.2. During the spray tests, fresh ECC was sprayed with air pressure of 100 psi (0.69 MPa). The distance between the spray gun and concrete surface was approximately 0.2 to 0.5 m, and the spray thickness was 20 mm. The mass of ECC attached to the concrete surface (m_1) and the mass of the rebound ECC (m_2) were obtained. The value of $m_2/(m_1 + m_2)$ was calculated as the rebound rate. It can be seen in Fig. 6 that both E-1.2 and E-2.2 could be pumped and sprayed, which further

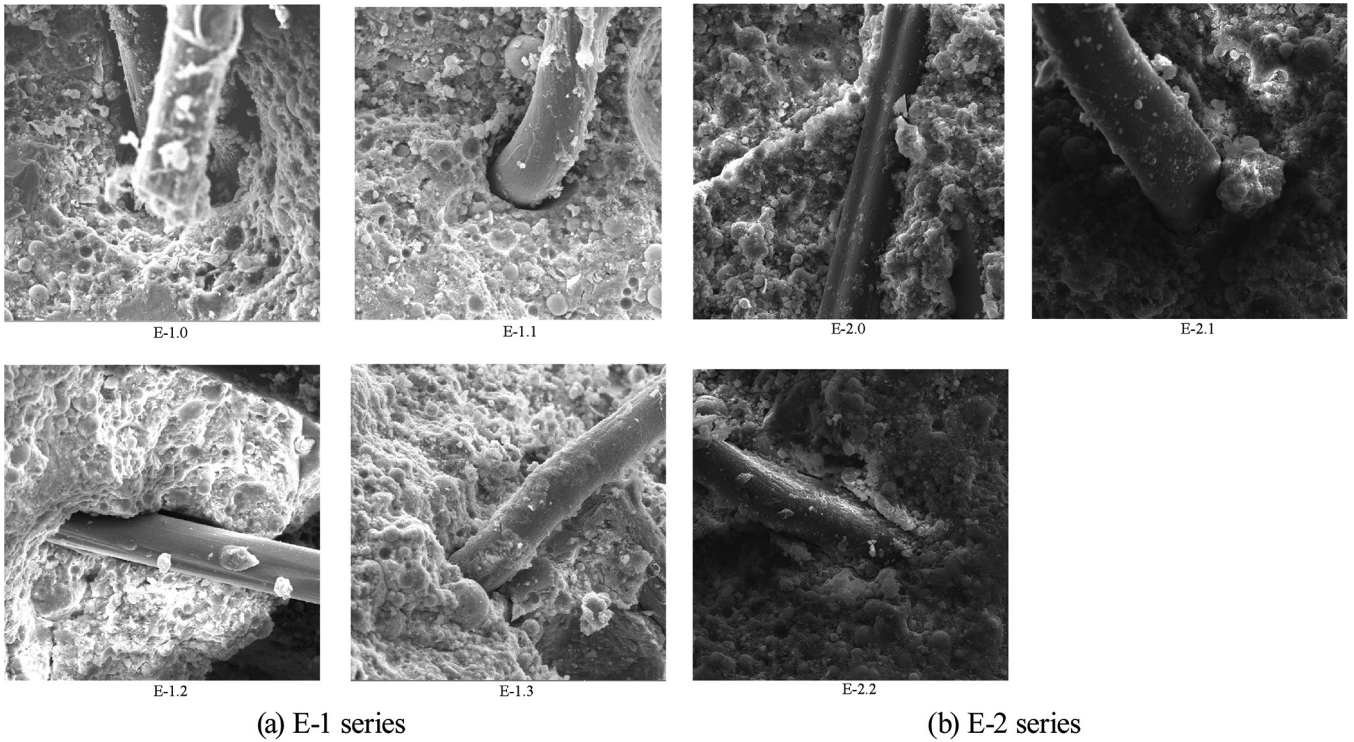


Fig. 5—SEM images of E-1 and E-2 series.



Fig. 6—Spray tests of: (left) E-1.2; and (right) E-2.2.

demonstrated the reliability of the workability evaluation indexes. However, the rebound rate of E-2.2 was 7.89% lower than that of E-1.2 (18.92%), indicating that E-2.2 had better workability.

In addition, a radar chart of all the issues regarding ECC material properties discussed is given in Fig. 7, which indicates that the mechanical properties, impermeability, and anti-drying-shrinkage ability of E-2.2 were better than those of E-1.2. Therefore, the E-2.2 ECC mixture proportions ($F/c = 4.44$, $SF/c = 0.20$, $SRA/c = 9\%$, and fiber volume content $V_f = 2\%$) having excellent workability (pumpability and sprayability), high toughness (the ultimate tensile strain ε_{tp} is greater than 3.5%), high tensile ductility achieved by forming multiple tight microcracks instead of localized large cracks (as shown in Fig. 8), good impermeability ($K = 1.713 \times 10^{-11} \text{ m/s} < 2.610 \times 10^{-11} \text{ m/s}$), and low drying

shrinkage strain ($\varepsilon_{st} = 603.6 \times 10^{-6} < 800 \times 10^{-6}$) were the final optimized ECC mixture proportions.

TOUGHNESS EVALUATION AND CHARACTERISTIC PARAMETERS CALIBRATION OF OPTIMIZED ECC

Toughness evaluation

Though the toughness evaluation of ECC could be carried out using the uniaxial tensile test, this method was complicated and time-consuming—advanced equipment was required and improper operation may have a great impact on test results. The operations of the four-point bending test were easy to conduct and are more widely used to evaluate the toughness of ECC. In addition, in tunnel engineering, direct shear failure caused by creep slip and dislocation of active faults will lead to tunnel lining cracking and even collapse of the whole structure, which seriously endangers

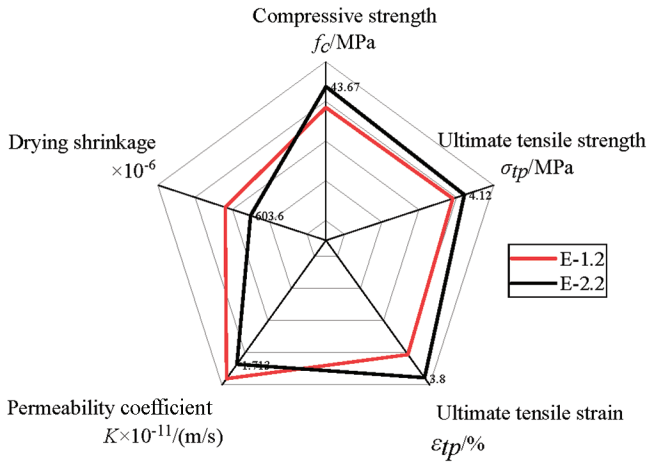


Fig. 7—Radar chart for PVA-ECC test results (E-1.2 and E-2.2).



Fig. 8—ECC multiple tight microcracks of E-2.2 direct tension test specimen.

the safety of the tunnel structure.⁴³ Thus, shear toughness is also a key parameter of ECC when used in underground and hydraulic engineering. Therefore, the toughness of the optimized ECC (E-2.2) was evaluated by combining the four-point bending test and the shear test.

Four-point bending tests were carried out according to ASTM C1609/C1609M-06,³⁹ and the flexural toughness was evaluated by the flexural toughness index (I_m) proposed by Naaman and Reinhardt.⁴⁴ The method stated in ASTM C1018 can only determine the toughness indexes I_5 , I_{10} , and I_{20} . However, Said and Razak⁴⁵ pointed out that toughness indexes I_5 , I_{10} , I_{20} , I_{30} , I_{40} , I_{50} , I_{60} , and I_{70} for ECC may be evaluated because of the high ductility and high deflection. Thus, according to the four-point bending test, the load-deflection relationship of E-2.2 shown in Fig. 9 and I_m and I_{MOR} can be calculated as follows

$$I_m = \int_0^{\frac{m+1}{2}} P(\delta)d\delta / \int_0^{\delta} P(\delta)d\delta = S_{OACD} / S_{OAB} \quad (3)$$

$$I_{MOR} = \int_0^{\delta_{MOR}} P(\delta)d\delta / \int_0^{\delta} P(\delta)d\delta = S_{OACEF} / S_{OAB} \quad (4)$$

where δ is the deflection of midspan at the first crack; the values of m were taken as 5, 10, 20, 30, 40, 50, 60, and 70,

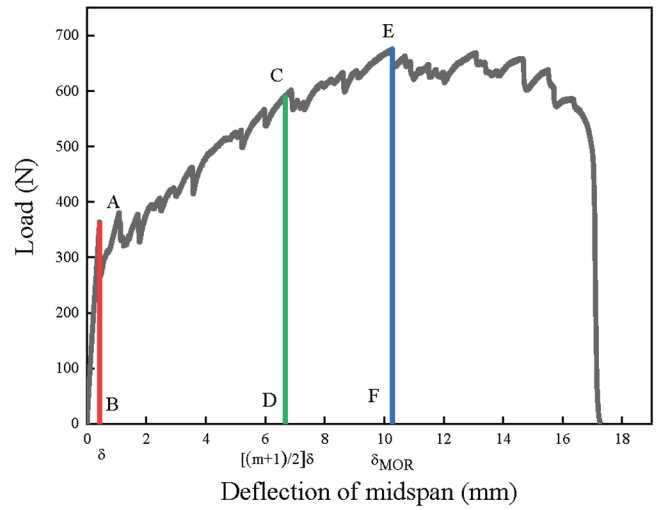


Fig. 9—Four-point bending test load-deflection curve (E-2.2).

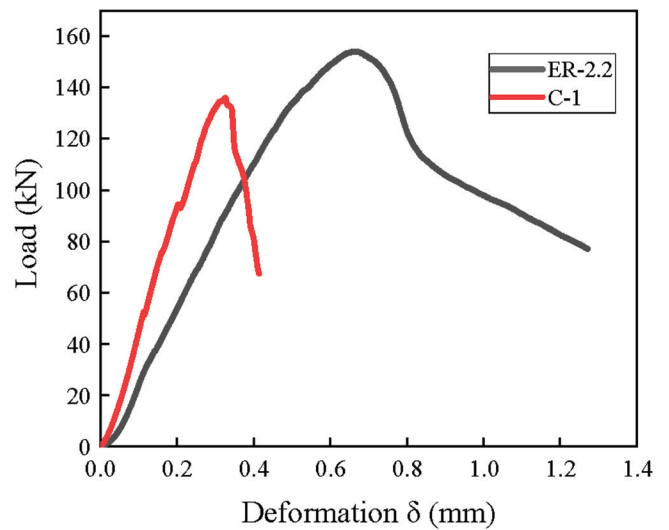


Fig. 10—Shear test load-deflection curves for E-2.2 and C-1.

respectively; and δ_{MOR} is the midspan deflection at ultimate load.

NC of the same f_c as E-2.2 was set as the control group named C-1, and the shear tests were carried out according to CECS 13-2009.⁴⁶ The shear test load-deflection curves of E-2.2 and C-1 are shown in Fig. 10. According to Deng et al.,⁴⁷ the shear toughness before peak load (T_p) and the shear toughness after peak load ($R_{p,k}$) can be calculated as follows

$$T_p = \Omega_p / 2bh^2 \quad (5)$$

$$R_{p,k} = \Omega_{p,k} / 2bh\delta_p k f_p \quad (6)$$

where Ω_p is the area under the load-deflection curve before the peak load; b and h are the width and height, respectively, of the shear specimen; δ_k is defined as K times δ_p ; δ_p is the deflection corresponding to peak load; K is taken as 1.2, 1.5, and 2.0, respectively⁴⁷; $\Omega_{p,k}$ is the area under the load-deflection curve from δ_p to δ_k ; and f_p is the shear strength.

Table 11—Test results of four-point bending and shear tests

Test	Toughness evaluation index	Test result	
		E-2.2	C-1
Four-point bending test	I_5	5.1	—
	I_{10}	10.5	—
	I_{20}	22.4	—
	I_{30}	35.1	—
	I_{40}	49.7	—
	I_{50}	67.8	—
	I_{60}	78.9	—
	I_{70}	91.3	—
	I_{MOR}	110.9	—
	$2\delta_{MOR}/(\delta - 1)$	78.0	—
Shear test	T_p	3.048%	0.269
	$R_{p,1.2}$	0.93	0.17
	$R_{p,1.5}$	0.82	0.08
	$R_{p,2.0}$	0.37	—

The test results of the bending and shear tests are given in Table 11.

Said and Razak⁴⁵ pointed out that ECC having toughness indexes $I_m > m$ and $I_{MOR} > 2\delta_{MOR}/(\delta - 1)$ can be termed as strain-hardening-type materials. It can be seen from Table 11 that with the increase of the m , the difference between the I_m and m increased. Meanwhile, I_{MOR} was 110.9, which was far greater than $2\delta_{MOR}/(\delta - 1) = 78.0$, indicating that the toughness of the material increases with the increase in deformation. The T_p and $R_{p,k}$ reflect the shear toughness of ECC; the larger the values, the greater the shear toughness.⁴⁷ The T_p of ECC was 3.672%, which was approximately 15 times that of C-1 ($T_p = 0.269$), and the maximum residual shear toughness of E-2.2 ($R_{p,1.2} = 0.93$) was approximately 12 times that of C-1 ($R_{p,1.5} = 0.08$).

Combined with the ultimate tensile strain obtained from the uniaxial tensile test in this paper, the complete toughness evaluation of E-2.2 was finally obtained, as shown in Table 12.

Material characteristic parameters

Also, according to the previous test results, the material characteristic parameters of E-2.2 are given in Table 13, including the density ρ , elastic modulus E_0 , uniaxial compression peak stress σ_{cp} and its corresponding strain ε_{cp} , uniaxial compression ultimate stress σ_{cu} , ultimate compression strain ε_{cu} , uniaxial tensile yield stress σ_{t0} and its yield strain ε_{t0} , ultimate tensile strength σ_{tp} and its corresponding strain ε_{tp} , as well as the tensile failure stress σ_{tu} and the failure strain ε_{tu} ; these provide a basis for its engineering application and numerical simulation. A comparison of the mechanical properties of E-2.2 and the traditional cement-based material C-1 used in underground and hydraulic engineering is given in Fig. 11, where the f_c was the same. It could be intuitively found that the radar chart of E-2.2 was fuller than that of C-1, indicating that ECC (E-2.2) had excellent mechanical

Table 12—Toughness evaluation indexes for E-2.2

Test	Toughness evaluation index	Test result
Uniaxial compression tests	ε_{cp}	0.416%
Uniaxial tensile tests	ε_{tp}	3.80%
Four-point bending test	I_5	5.1
	I_{10}	10.5
	I_{20}	22.4
	I_{30}	35.1
	I_{40}	49.7
	I_{50}	67.8
	I_{60}	78.9
	I_{70}	91.3
	I_{MOR}	110.9
	Shear test	T_p
$R_{p,1.2}$		0.93
$R_{p,1.5}$		0.82
$R_{p,2.0}$		0.37

Table 13—Material characteristic parameters for E-2.2

Characteristic parameter	Value
E_0 , MPa	22.60
σ_{cp} , MPa	43.67
ε_{cp} , %	0.416
σ_{cu} , MPa	7.95
ε_{cu} , %	3.91
σ_{t0} , MPa	3.53
ε_{t0} , %	0.016
σ_{tp} , MPa	4.12
ε_{tp} , %	3.80
σ_{tu} , MPa	1.02
ε_{tu} , %	4.50
Density, kg/m ³	1950

properties compared with the NC (C-1), especially for toughness.

CONCLUSIONS

To meet the requirements of underground hydraulic structures, an engineered cementitious composite (ECC) mixture ratio with a high water-cement ratio (w/c) and high fly ash (FA) content was adopted, and silica fume (SF) and shrinkage-reducing agent (SRA) were added to improve the ECC's performance. The conclusions of this study are summarized as follows:

1. High-FA ECC mixture proportions were adapted in this study. FA not only replaced a large portion of cement in ECC without sacrificing its mechanical properties and tensile ductility but also offered environmental advantages in processing cement.

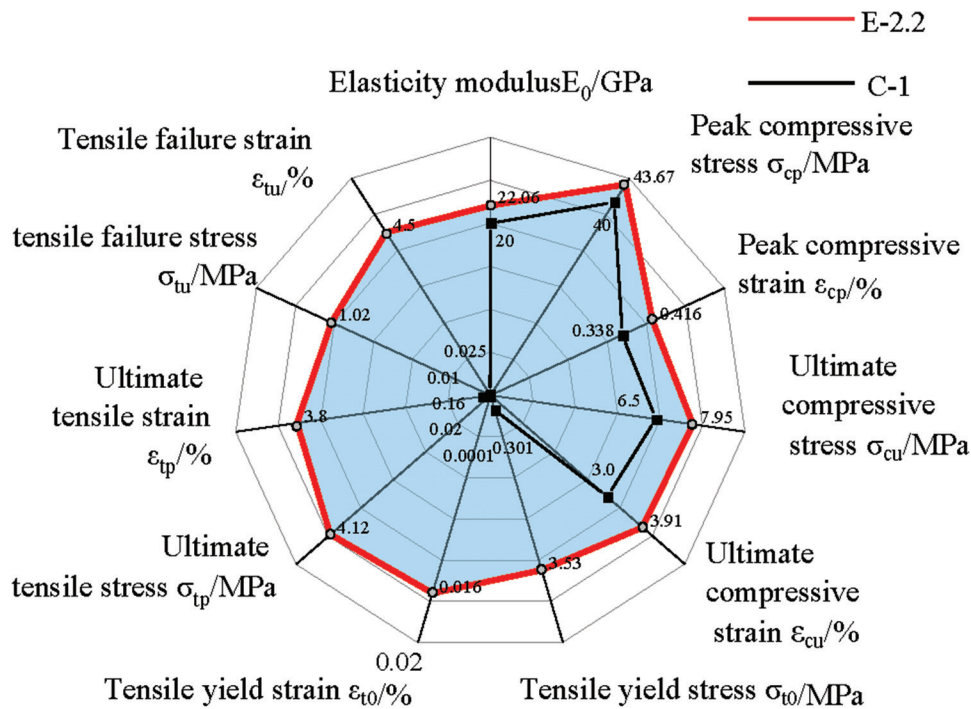


Fig. 11—Radar chart for PVA-ECC characteristic material parameters (E-2.2).

2. The workability evaluation indexes of fresh ECC were obtained, of which the slump S_L was in the range of 140 to 200 mm to ensure proper fluidity; the slump flow S_f was in the range of 400 to 600 mm; and funnel flow time t was 4 to 10 seconds to ensure cohesion; and the ratio of slump to slump flow (S_L/S_f) was generally approximately 0.45 to ensure the balance between fluidity and cohesion.

3. An ECC mixture proportion (E-2.2), with excellent workability (pumpability and sprayability), high toughness (the ultimate tensile strain ϵ_{tp} is greater than 3.5%), good impermeability (permeability coefficient $K = 1.713 \times 10^{-11} \text{ m/s} < 2.610 \times 10^{-11} \text{ m/s}$), and low drying shrinkage strain (drying shrinkage strain $\epsilon_{st} = 603.6 \times 10^{-6} < 686.5 \times 10^{-6}$) was the result of the final optimization.

4. The use of SF can effectively improve both pumpability and sprayability of high- w/c ECC. The S_L decreased gradually with the increase of SF content, indicating that the fluidity decreases gradually. However, the S_f decreased and the t increased, indicating that the cohesion increases.

5. The more SF added, the lower the K value that could be achieved. Adding SF could increase the density of the cement matrix. The ECC porosity and pore density decreased with the increase of SF content.

6. Combined with the four-point bending test and shear test, the complete toughness evaluation for E-2.2 was established; the material characteristic parameters of E-2.2 are given in Table 13, which can be directly applied to future engineering.

AUTHOR BIOS

Xiaoqin Li is a Professor in the Faculty of Civil Engineering and Mechanics at Kunming University of Science and Technology. She received her BS from Tsinghua University, Beijing, China, and her MS and PhD from The University of Edinburgh, Edinburgh, UK. Her research interests include ECCs and fiber-reinforced polymer (FRP)-strengthened structures.

Li Zhang is a Postgraduate Student in the Faculty of Civil Engineering and Mechanics at Kunming University of Science and Technology, Kunming, Yunnan, China. Her research interests include engineered cementitious composites (ECCs) and structural engineering.

Wenlu Wen is a Manager of QuakeSafe Technologies Co., Ltd., Kunming, Yunnan, China.

Shihua Li is a Director of YCIH Green High-Performance Concrete Company Limited, Kunming, Yunnan, China.

Xu Zhou is a Graduate Student in the Faculty of Civil Engineering and Mechanics at Kunming University of Science and Technology. His research interests include ECCs and structural engineering.

ACKNOWLEDGMENTS

The authors gratefully acknowledge the funding support of the National Natural Science Foundation of China (Grant No. 52168028, 51968035) and Yunnan Youth Talent Project (No. [2020]150 YNWR-QNBJ-2020-049).

REFERENCES

- Li, V. C., "Tailoring ECC for Special Attributes: A Review," *International Journal of Concrete Structures and Materials*, V. 6, No. 3, 2012, pp. 135-144.
- Kim, Y. Y.; Fischer, G.; and Li, V. C., "Performance of Bridge Deck Link Slabs Designed with Ductile Engineered Cementitious Composite," *ACI Structural Journal*, V. 101, No. 6, Nov.-Dec. 2004, pp. 792-801.
- Lee, C.-H.; Chiu, Y.-C.; Wang, T.-T.; and Huang, T.-H., "Application and Validation of Simple Image-Mosaic Technology for Interpreting Cracks on Tunnel Lining," *Tunnelling and Underground Space Technology*, V. 34, 2013, pp. 61-72. doi: 10.1016/j.tust.2012.11.002
- Mashimo, H.; Isago, N.; Kitani, T.; and Endou, T., "Effect of Fiber Reinforced Concrete on Shrinkage Crack of Tunnel Lining," *Tunnelling and Underground Space Technology*, V. 21, No. 3-4, 2006, pp. 382-383. doi: 10.1016/j.tust.2005.12.194
- Liu, H.; Zhang, Q.; Gu, C.; Su, H.; and Li, V. C., "Influence of Micro-Cracking on the Permeability of Engineered Cementitious Composites," *Cement and Concrete Composites*, V. 72, 2016, pp. 104-113. doi: 10.1016/j.cemconcomp.2016.05.016
- FERC, "Engineering Guidelines for the Evaluation of Hydropower Projects," Office of Hydropower Licensing, Federal Energy Regulatory Commission, Washington, DC, 2013, <https://www.ferc.gov/industries-data/hydropower/dam-safety-and-inspections/eng-guidelines>. (last accessed Nov. 16, 2023)

7. Zhou, J.; Qian, S.; Ye, G.; Copuroglu, O.; van Breugel, K.; and Li, V. C., "Improved Fiber Distribution and Mechanical Properties of Engineered Cementitious Composites by Adjusting the Mixing Sequence," *Cement and Concrete Composites*, V. 34, No. 3, 2012, pp. 342-348. doi: 10.1016/j.cemconcomp.2011.11.019
8. Lepech, M. D., and Li, V. C., "Water Permeability of Engineered Cementitious Composites," *Cement and Concrete Composites*, V. 31, No. 10, 2009, pp. 744-753. doi: 10.1016/j.cemconcomp.2009.07.002
9. Yang, E.-H.; Yang, Y.; and Li, V. C., "Use of High Volumes of Fly Ash to Improve ECC Mechanical Properties and Material Greenness," *ACI Materials Journal*, V. 104, No. 6, Nov.-Dec. 2007, pp. 620-628.
10. Sherir, M. A. A.; Hossain, K. M. A.; and Lachemi, M., "Structural Performance of Polymer Fiber Reinforced Engineered Cementitious Composites Subjected to Static and Fatigue Flexural Loading," *Polymers*, V. 7, No. 7, 2015, pp. 1299-1330. doi: 10.3390/polym7071299
11. Wang, S., and Li, V. C., "Engineered Cementitious Composites with High-Volume Fly Ash," *ACI Materials Journal*, V. 104, No. 3, May-June 2007, pp. 233-241.
12. Qian, C. X., and Stroeven, P., "Development of Hybrid Polypropylene-Steel Fibre-Reinforced Concrete," *Cement and Concrete Research*, V. 30, No. 1, 2000, pp. 63-69. doi: 10.1016/S0008-8846(99)00202-1
13. Şahmaran, M., and Li, V. C., "Durability Properties of Micro-Cracked ECC Containing High Volumes Fly Ash," *Cement and Concrete Research*, V. 39, No. 11, 2009, pp. 1033-1043. doi: 10.1016/j.cemconres.2009.07.009
14. Zhang, X.; Liu, S.; Yan, C.; Wang, X.; and Wang, H., "Effects of Traffic Vibrations on the Flexural Properties of Newly Placed PVA-ECC Bridge Repairs," *Materials (Basel)*, V. 12, No. 20, 2019, Article No. 3337. doi: 10.3390/ma12203337
15. Marks, J., and Conklin, J., "Engineered Cementitious Composites: Applications and Impact of High Tensile, Self-Healing Concrete," University of Pittsburgh Swanson School of Engineering, Pittsburgh, PA, Session A5, 2013, Paper No. 3204.
16. Bäuml, M. F., and Wittmann, F. H., "Application of PVA-Fiber Reinforced Self-Compacting Concrete (ECC) for Repair of Concrete Structures," *Restoration of Buildings and Monuments*, V. 8, No. 6, 2002, pp. 591-604. doi: 10.1515/rbm-2002-5709
17. Cui, L., and Cahyadi, J. H., "Permeability and Pore Structure of OPC Paste," *Cement and Concrete Research*, V. 31, No. 2, 2001, pp. 277-282. doi: 10.1016/S0008-8846(00)00474-9
18. Li, V. C.; Mishra, D. K.; and Wu, H.-C., "Matrix Design for Pseudo-Strain-Hardening Fibre Reinforced Cementitious Composites," *Materials and Structures*, V. 28, No. 10, 1995, pp. 586-595. doi: 10.1007/BF02473191
19. Gao, S.; Wang, Z.; Wang, W.; and Qiu, H., "Effect of Shrinkage-Reducing Admixture and Expansive Agent on Mechanical Properties and Drying Shrinkage of Engineered Cementitious Composite (ECC)," *Construction and Building Materials*, V. 179, 2018, pp. 172-185. doi: 10.1016/j.conbuildmat.2018.05.203
20. GB 50108-2008, "Technical Code for Waterproofing of Underground Works," Ministry of Housing and Urban-Rural Development of the People's Republic of China, Beijing, China, 2008.
21. Zhang, P., and Li, Q., "Effect of Polypropylene Fiber on Durability of Concrete Composite Containing Fly Ash and Silica Fume," *Composites Part B: Engineering*, V. 45, No. 1, 2013, pp. 1587-1594. doi: 10.1016/j.compositesb.2012.10.006
22. Hamami, A. A.; Turcry, P.; and Ait-Mokhtar, A., "Influence of Mix Proportions on Microstructure and Gas Permeability of Cement Pastes and Mortars," *Cement and Concrete Research*, V. 42, No. 2, 2012, pp. 490-498. doi: 10.1016/j.cemconres.2011.11.019
23. Pereira, C. G.; Castro-Gomes, J.; and Pereira de Oliveira, L., "Influence of Natural Coarse Aggregate Size, Mineralogy and Water Content on the Permeability of Structural Concrete," *Construction and Building Materials*, V. 23, No. 2, 2009, pp. 602-608. doi: 10.1016/j.conbuildmat.2008.04.009
24. Niu, Q.; Feng, N.; Yang, J.; and Zheng, X., "Effect of Superfine Slag Powder on Cement Properties," *Cement and Concrete Research*, V. 32, No. 4, 2002, pp. 615-621. doi: 10.1016/S0008-8846(01)00730-X
25. Heikal, M.; El-Didamony, H.; and Morsy, M. S., "Limestone-Filled Pozzolanic Cement," *Cement and Concrete Research*, V. 30, No. 11, 2000, pp. 1827-1834. doi: 10.1016/S0008-8846(00)00402-6
26. Lee, C.-L.; Huang, R.; Lin, W.-T.; and Weng, T.-L., "Establishment of the Durability Indices for Cement-Based Composite Containing Supplementary Cementitious Materials," *Materials & Design*, V. 37, 2012, pp. 28-39. doi: 10.1016/j.matdes.2011.12.030
27. Yang, C. C., and Chiang, C. T., "On the Relationship between Pore Structure and Charge Passed from RCPT in Mineral-Free Cement-Based Materials," *Materials Chemistry and Physics*, V. 93, No. 1, 2005, pp. 202-207. doi: 10.1016/j.matchemphys.2005.03.044
28. Ding, Z.; Wen, J.; Li, X.; and Yang, X., "Permeability of the Bonding Interface between Strain-Hardening Cementitious Composite and Normal Concrete," *AIP Advances*, V. 9, No. 5, 2019, Article No. 055107. doi: 10.1063/1.5086915
29. Li, X.; Yang, X.; Ding, Z.; Du, X.; and Wen, J., "ECC Design Based on Uniform Design Test Method and Alternating Conditional Expectation," *Mathematical Problems in Engineering*, V. 2019, 2019, Article No. 9575897. doi: 10.1155/2019/9575897
30. Wu, Z. W., and Lian, H. Z., *High Performance Concrete*, Railway Publishing House, Beijing, China, 2008.
31. Rajabipour, F.; Sant, G.; and Weiss, J., "Interactions between Shrinkage Reducing Admixtures (SRA) and Cement Paste's Pore Solution," *Cement and Concrete Research*, V. 38, No. 5, 2008, pp. 606-615. doi: 10.1016/j.cemconres.2007.12.005
32. Thomas, M. D. A.; Hooton, R. D.; Scott, A.; and Zibara, H., "The Effect of Supplementary Cementitious Materials on Chloride Binding in Hardened Cement Paste," *Cement and Concrete Research*, V. 42, No. 1, 2012, pp. 1-7. doi: 10.1016/j.cemconres.2011.01.001
33. Ngo, T.-T.; Kadri, E.-H.; Cussigh, F.; and Bennacer, R., "Relationships between Concrete Composition and Boundary Layer Composition to Optimise Concrete Pumpability," *European Journal of Environmental and Civil Engineering*, V. 16, No. 2, 2012, pp. 157-177. doi: 10.1080/19648189.2012.666910
34. JGJ/T 10-2011, "Technical Specification for Construction of Concrete Pumping," Ministry of Housing and Urban-Rural Development of the People's Republic of China, Beijing, China, 2011.
35. JGJ/T 372-2016, "Technical Specification for Application of Sprayed Concrete," Ministry of Housing and Urban-Rural Development of the People's Republic of China, Beijing, China, 2016.
36. Kim, Y. Y.; Kong, H.-J.; and Li, V. C., "Design of Engineered Cementitious Composite Suitable for Wet-Mixture Shotcreting," *ACI Materials Journal*, V. 100, No. 6, Nov.-Dec. 2003, pp. 511-518.
37. Yun, K.-K.; Choi, S.-Y.; and Yeon, J. H., "Effects of Admixtures on the Rheological Properties of High-Performance Wet-Mix Shotcrete Mixtures," *Construction and Building Materials*, V. 78, 2015, pp. 194-202.
38. Shi, Y.; Matsui, I.; and Feng, N., "Effect of Compound Mineral Powders on Workability and Rheological Property of HPC," *Cement and Concrete Research*, V. 32, No. 1, 2002, pp. 71-78. doi: 10.1016/S0008-8846(01)00631-7
39. ASTM C1609/C1609M-06, "Standard Test Method for Flexural Performance of Fiber-Reinforced Concrete (Using Beam With Third-Point Loading)," ASTM International, West Conshohocken, PA, 2006, 8 pp.
40. GB/T 50082-2009, "Standard for Test Methods of Long-Term Performance and Durability of Ordinary Concrete," Ministry of Housing and Urban-Rural Development of the People's Republic of China, Beijing, China, 2009.
41. Zhang, J.; Gong, C.; Guo, Z.; and Zhang, M., "Engineered Cementitious Composite with Characteristic of Low Drying Shrinkage," *Cement and Concrete Research*, V. 39, No. 4, 2009, pp. 303-312. doi: 10.1016/j.cemconres.2008.11.012
42. Abd Elrahman, M., and Hillemeier, B., "Combined Effect of Fine Fly Ash and Packing Density on the Properties of High Performance Concrete: An Experimental Approach," *Construction and Building Materials*, V. 58, 2014, pp. 225-233. doi: 10.1016/j.conbuildmat.2014.02.024
43. Shahidi, A. R., and Vafaeian, M., "Analysis of Longitudinal Profile of the Tunnels in the Active Faulted Zone and Designing the Flexible Lining (for Koohrang-III Tunnel)," *Tunnelling and Underground Space Technology*, V. 20, No. 3, 2005, pp. 213-221. doi: 10.1016/j.tust.2004.08.003
44. Naaman, A., and Reinhardt, H., "Characterization of High Performance Fiber Reinforced Cement Composites - HPRFCC," *High Performance Fiber Reinforced Cement Composites 2 (HPRFCC 2): Proceedings of the Second International RILEM Workshop*, Taylor & Francis, London, UK, 1996, pp. 1-24.
45. Said, S. H., and Razak, H. A., "The Effect of Synthetic Polyethylene Fiber on the Strain Hardening Behavior of Engineered Cementitious Composite (ECC)," *Materials & Design*, V. 86, 2015, pp. 447-457. doi: 10.1016/j.matdes.2015.07.125
46. CECS 13-2009, "Standard Test Method for Fiber Reinforced Concrete," China Association of Engineering and Construction Standardization, Beijing, China, 2009.
47. Deng, M.; Liu, H.; Ma, F.; and Deng, C., "Double Shear Experiment of Highly Ductile Concrete Modified by Polyvinyl Alcohol and Shear Toughness Evaluation Method," *Acta Materiae Compositae Sinica*, V. 37, No. 2, 2020, pp. 461-471.

NOTES:
